ESAIM: M2AN 57 (2023) 2077–2095
https://doi.org/10.1051/m2an/2023044

ESAIM: Mathematical Modelling and Numerical Analysis
www.esaim-m2an.org

A HYBRID-DG METHOD FOR SINGULARLY PERTURBED CONVECTION-DIFFUSION EQUATIONS ON PIPE NETWORKS

Herbert Egger[1,2] and Nora Philippi[2,*]

Abstract. We study the numerical approximation of singularly perturbed convection-diffusion problems on one-dimensional pipe networks. In the vanishing diffusion limit, the number and type of boundary conditions and coupling conditions at network junctions change, which gives rise to singular layers at the outflow boundaries of the pipes. A hybrid discontinuous Galerkin method is proposed, which provides a natural upwind mechanism for the convection-dominated case. Moreover, the method provides a viable approximation for the limiting pure transport problem. A detailed analysis of the singularities of the solution and the discretization error is presented, and an adaptive strategy is proposed, leading to order optimal error estimates that hold uniformly in the singular perturbation limit. The theoretical results are confirmed by numerical tests.

Mathematics Subject Classification. 35B25, 35B40, 35K20, 35R02, 65N30, 76R99.

Received September 9, 2022. Accepted May 16, 2023.

1. Introduction

We are interested in the numerical solution of convection-diffusion processes on one-dimensional pipe networks. Such problems describe, *e.g.*, the contaminant transport in water supply networks and systems of 1D-cracks [20, 23], or the distribution of energy in district heating networks [17]. Related nonlinear problems have been studied in the context of traffic flow modeling; see [14] for an introduction.

Problem setting and asymptotic analysis. On every single pipe of the network, the transport of matter is described by the convection-diffusion problem

$$\partial_t u^\varepsilon + b\partial_x u^\varepsilon = \varepsilon \partial_{xx} u^\varepsilon, \qquad x \in (0,\ell),\ t > 0, \tag{1}$$

$$u^\varepsilon = \hat{g}, \qquad x \in \{0,\ell\},\ t > 0. \tag{2}$$

Here, u^ε denotes the quantity of interest, *e.g.*, the concentration of the contaminant, $b > 0$ is the flow velocity, $\varepsilon > 0$ is the diffusion coefficient, and $\hat{g}$ is suitable boundary data. In the vanishing diffusion limit $\varepsilon \to 0$, the boundary condition at $x = \ell$ becomes obsolete. This leads to a boundary layer for $0 < \varepsilon \ll 1$ accompanied by

Keywords and phrases. Singular perturbation problems, vanishing diffusion limit, discontinuous Galerkin methods, asymptotic analysis, parameter robust error estimates.

[1] Institute for Numerical Mathematics, Johannes-Kepler University Linz, Linz, Austria.
[2] Johann Radon Institute for Computational and Applied Mathematics, Linz, Austria.
*Corresponding author: nora.philippi@ricam.oeaw.ac.at

© The authors. Published by EDP Sciences, SMAI 2023

This is an Open Access article distributed under the terms of the Creative Commons Attribution License (https://creativecommons.org/licenses/by/4.0), which permits unrestricted use, distribution, and reproduction in any medium, provided the original work is properly cited.

a blow-up of the derivatives of the solution, which can be expressed by

$$\|u^\varepsilon\|_{L^\infty(0,t_{\max};H^1(0,\ell))} \approx C/\sqrt{\varepsilon}. \tag{3}$$

In contrast to that, the solution u° of the transport problem, which arises in the limit $\varepsilon = 0$, may be perfectly smooth within the pipe, although violating the boundary condition at $x = \ell$. Maximum principles allow us to verify that both, u^ε and u°, are bounded uniformly, and under appropriate assumptions, one can further show that

$$\|u^\varepsilon - u^\circ\|_{L^\infty(0,t_{\max};L^2(0,\ell))} \le C\sqrt{\varepsilon} \tag{4}$$

with a uniform constant C; see *e.g.*, [27]. This asymptotic estimate suggests that the transport solution u° may serve as a good approximation for u^ε for small $0 < \varepsilon \ll 1$.

Extension to networks. Additional coupling conditions are required to model the flow through junctions of more than two pipes and to determine the values $\hat{g}$ in (2) at internal junctions. The number and type of these conditions may change in the singular limit $\varepsilon \to 0$, which gives rise to additional interior layers. As elaborated in [11], the blow-up of the solution and the asymptotic estimates for a single pipe, however, carry over almost verbatim to the network setting. We refer to [16] for results concerning a general class of coupling conditions and to [2] for related investigations concerning optimal control. Vanishing diffusion limits for scalar conservation laws in traffic networks are studied in [5].

Numerical approximation. The discretization of singularly perturbed convection-diffusion problems is well studied in the literature; see [27] for a comprehensive survey. A key ingredient for the robust approximation is the use of layer-adapted meshes. Finite element approximations on Shishkin-type meshes were investigated in [6,9,25,26]; also see [28] for the analysis of higher-order schemes and [30,33] for the investigation of discontinuous Galerkin methods on various layer-adapted meshes. In this paper, we consider the spatial approximation by a *hybrid discontinuous Galerkin* (dG) method; see [4,7] for background material. Related methods for problems on multi-dimensional domains were investigated in [12,13,22] and by Chen *et al.* [3] in the context of optimal control.

Main contributions. The proposed hybrid-dG method not only provides an upwind mechanism for handling the convection-dominated regime but, more importantly, allows a natural treatment of the coupling conditions at pipe junctions. In the singular limit $\varepsilon = 0$, the method then reduces to the hybrid-dG scheme for pure transport on networks, which has been analyzed in [10]. By the extension of previous results, we will establish uniform error estimates, which for a single pipe and approximations of order k take the form

$$\|u^\varepsilon - \tilde{u}_h^\varepsilon\|_{L^\infty(0,T;L^2(0,\ell))} \le C \max\big(h^{k+1}, \min\big(\sqrt{\varepsilon}, h^k\big)\big). \tag{5}$$

The constant C here only depends on the regularity of the boundary data but is independent of ε and h. The approximation $\tilde{u}_h^\varepsilon$ will be chosen adaptively as

$$\tilde{u}_h^\varepsilon = \begin{cases} u_h^\varepsilon, & \varepsilon \ge h^{2k}, \\ u_h^\circ, & \varepsilon < h^{2k}, \end{cases}$$

where u_h^ε is the hybrid-dG approximation for the convection-diffusion problem on a layer-adapted mesh $\mathcal{T}_h^\varepsilon$ of Gartland-type [15], while u_h° is the hybrid-dG approximation [10] for the pure transport problem on a uniform mesh $\mathcal{T}_h^\circ$. Following [15,26], the mesh $\mathcal{T}_h^\varepsilon$ is chosen uniformly in the interval $(0, x^*(\varepsilon))$ away from the layer, and geometrically refined within the layer $(x^*(\varepsilon), \ell)$. As transition point, we will choose

$$x^*(\varepsilon) \approx \varepsilon \log(1/\varepsilon) \lesssim \varepsilon \log(1/h); \tag{6}$$

the second inequality only holds due to the condition $\varepsilon \ge h^{2k}$. Using this observation, one can show that the number of elements in $\mathcal{T}_h^\varepsilon$ is of optimal order, *i.e.*, $N \approx h^{-1}$. At the same time, the choice of the transition point

$x^*(\varepsilon)$ simplifies the convergence analysis significantly; see Section 4.3. For $\varepsilon < h^{2k}$ the solution to the convection-diffusion problem is close enough to the corresponding transport solution which is smooth. Moreover, the layer region is very small, and hence a good approximation can be found already by the hybrid-dG method for the pure transport problem on a uniform mesh $\mathcal{T}_h^\circ$. Let us note that $\mathcal{T}_h^\circ$ is a coarser mesh than $\mathcal{T}_h^\varepsilon$, which is refined within the layer in order to guarantee discrete stability for small but not negligible diffusion. Our results cover the case of a single pipe as well as finite networks of pipes of a rather general topology, in particular, including cycles. Different regimes, *i.e.*, transport- or diffusion-dominated, for different pipes can be handled naturally. Similar uniform convergence estimates also hold for fully discrete schemes obtained after time discretization by appropriate time-stepping schemes, which will be demonstrated in numerical tests.

Outline. In Section 2, we introduce our notation and main assumptions, state the convection-diffusion and pure transport problems on networks, and then summarize some important properties of their solutions. The hybrid-dG method is proposed in Section 3, and we state a preliminary error estimate. Section 4 contains our main convergence result and its proof. For completeness of the presentation, the proofs of some auxiliary technical results are included in the appendix. In order to illustrate our theoretical results, we give numerical tests in Section 5. The presentation closes with a short summary and remarks concerning possible extensions of our results.

2. Problem statement

Let us start by introducing the relevant notation and then give a complete definition of the problems under consideration. After that, we state the main assumptions for our analysis and summarize the basic properties of solutions to the continuous problems.

2.1. Notation

Following [10,21], the network topology is described by a finite, directed, and connected graph $\mathcal{G} = (\mathcal{V}, \mathcal{E})$, with vertices $\mathcal{V} = \{v_1, \dots, v_n\}$ and edges $\mathcal{E} = \{e_1, \dots, e_m\} \subset \mathcal{V} \times \mathcal{V}$. We write $\mathcal{E}(v) = \{e \in \mathcal{E} : e = (v, \cdot) \text{ or } e = (\cdot, v)\}$ for the set of edges incident to a vertex $v \in \mathcal{V}$, and $\mathcal{V}_\partial = \{v \in \mathcal{V} : |\mathcal{E}(v)| = 1\}$, $\mathcal{V}_0 = \mathcal{V} \backslash \mathcal{V}_\partial$ for the sets of boundary and internal vertices. As usual, $|S|$ describes the cardinality of a finite set S. For any edge $e = (v^{\mathrm{in}}, v^{\mathrm{out}})$, we define two values

$$n_e(v^{\mathrm{in}}) := -1 \quad \text{and} \quad n_e(v^{\mathrm{out}}) := 1$$

indicating the start and end point of the edge, and we set $n_e(v) := 0$ for $v \in \mathcal{V} \backslash \{v^{\mathrm{in}}, v^{\mathrm{out}}\}$. We write $\mathcal{E}^{\mathrm{in}}(v) := \{e \in \mathcal{E} : n_e(v) > 0\}$ and $\mathcal{E}^{\mathrm{out}}(v) := \{e \in \mathcal{E} : n_e(v) < 0\}$ for the sets of edges pointing into and out of the vertex $v \in \mathcal{V}$, respectively. Furthermore, we split $\mathcal{V}_\partial$ into a set of boundary vertices $\mathcal{V}_\partial^{\mathrm{in}} := \{v \in \mathcal{V}_\partial : n_e(v) < 0 \text{ for } e \in \mathcal{E}(v)\}$, from which edges leave into the network, and the complement $\mathcal{V}_\partial^{\mathrm{out}} := \{v \in \mathcal{V}_\partial : b_e n_e(v) > 0 \text{ for } e \in \mathcal{E}(v)\}$, in which edges terminate; see Figure 1 for an illustration. To any edge $e \in \mathcal{E}$, we associate a length ℓ_e, and identify $e \simeq (0, \ell_e)$ with an interval. By $L^2(e) = L^2(0, \ell_e)$ and

$$L^2(\mathcal{E}) = L^2(e_1) \times \cdots \times L^2(e_m) = \big\{u : u_e \in L^2(e) \text{ for all } e \in \mathcal{E}\big\},$$

we designate the spaces of square-integrable functions on a pipe e and the network $\mathcal{E}$, respectively, and we write $u_e = u|_e$ for the restriction of u to the edge e. The norm and scalar product for the space $L^2(\mathcal{E})$ are given by

$$\|u\|_{L^2(\mathcal{E})}^2 = \sum_{e \in \mathcal{E}} \|u_e\|_{L^2(e)}^2 \qquad \text{and} \qquad (u, w)_{L^2(\mathcal{E})} = \sum_{e \in \mathcal{E}} (u_e, w_e)_{L^2(e)}.$$

We further define the broken Sobolev spaces

$$H_{pw}^k(\mathcal{E}) = \big\{u \in L^2(\mathcal{E}) : u_e \in H^k(e) \text{ for all } e \in \mathcal{E}\big\}, \qquad k \geq 0.$$

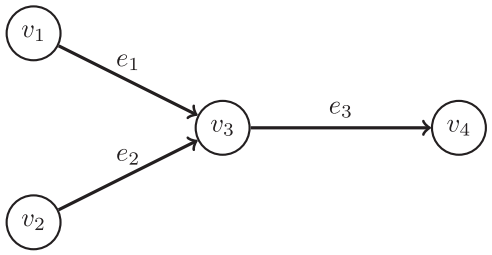

FIGURE 1. Network with edges $e_1 = (v_1, v_3)$, $e_2 = (v_2, v_3)$, and $e_3 = (v_3, v_4)$, inner vertex $\mathcal{V}_0 = \{v_3\}$, and boundary vertices $\mathcal{V}_\partial = \{v_1, v_2, v_4\}$. The set $\mathcal{E}(v_3) = \{e_1, e_2, e_3\}$ contains all edges incident to the vertex v_3. This set can be split into $\mathcal{E}^{\text{in}}(v_3) = \{e_1, e_2\}$ and $\mathcal{E}^{\text{out}}(v_3) = \{e_3\}$ with the edges that point into or out of the vertex v_3, respectively. The boundary vertices are split into $\mathcal{V}_\partial^{\text{in}} = \{v_1, v_2\}$ and $\mathcal{V}_\partial^{\text{out}} = \{v_4\}$ containing the vertices from which edges originate or in which edges terminate.

Note that $H^0_{pw}(\mathcal{E}) = L^2(\mathcal{E})$ and for $k \geq 1$ the functions $u \in H^k_{pw}(\mathcal{E})$ are continuous along edges $e \in \mathcal{E}$, but may be discontinuous across junctions $v \in \mathcal{V}_0$. The sub-space of functions that are continuous also across junctions is denoted by $H^1(\mathcal{E})$. Any $u \in H^1(\mathcal{E})$ has unique values $u(v)$ for every $v \in \mathcal{V}$, and we write $\ell_2(\mathcal{V})$ for the space of possible vertex values.

2.2. Convection-diffusion problem

We are now in the position to introduce the parabolic problem for $\varepsilon > 0$. Along the pipes of the network, we assume

$$\partial_t u_e^\varepsilon(x,t) + b_e \partial_x u_e^\varepsilon(x,t) = \varepsilon \partial_{xx} u_e^\varepsilon(x,t), \qquad x \in e,\ e \in \mathcal{E},\ t > 0. \tag{7}$$

Like on a single pipe, we enforce Dirichlet conditions at the boundary vertices, *i.e.*,

$$u^\varepsilon(v,t) = \hat{g}_v(t), \qquad v \in \mathcal{V}_\partial,\ t > 0. \tag{8}$$

At the interior vertices $v \in \mathcal{V}_0$, on the other hand, we require the coupling conditions

$$u_e^\varepsilon(v,t) = \hat{u}_v^\varepsilon(t), \qquad v \in \mathcal{V}_0,\ e \in \mathcal{E}(v),\ t > 0, \tag{9}$$

$$\sum_{e \in \mathcal{E}(v)} (b_e u_e^\varepsilon(v,t) - \varepsilon \partial_x u_e^\varepsilon(v,t)) n_e(v) = 0, \qquad v \in \mathcal{V}_0,\ t > 0, \tag{10}$$

which encode continuity of the density u^ε and conservation of mass across network junctions. The conditions (9) and (10) make up $|\mathcal{E}(v)| + 1$ coupling conditions at each interior vertex $v \in \mathcal{V}_0$, corresponding to the number of all incident edges and the additional unknown vertex value $\hat{u}_v^\varepsilon$, which is called *hybrid variable* in the following.

2.3. Limiting transport problem

In the vanishing diffusion limit $\varepsilon = 0$, the flow on the pipes is described by the hyperbolic transport equation

$$\partial_t u_e^\circ(x,t) + b_e \partial_x u_e^\circ(x,t) = 0, \qquad x \in e,\ e \in \mathcal{E},\ t > 0. \tag{11}$$

We can now prescribe Dirichlet data only at the inflow boundary vertices, *i.e.*,

$$u_e^\circ(v,t) = \hat{g}_v(t), \qquad v = \mathcal{V}_\partial^{\text{in}},\ t > 0. \tag{12}$$

The coupling across network junctions is further described by

$$u_e^\circ(v,t) = \hat{u}_v^\circ(t), \qquad v \in \mathcal{V}_0,\ e \in \mathcal{E}^{\mathrm{out}}(v),\ t > 0, \tag{13}$$

$$\sum_{e\in\mathcal{E}^{\mathrm{in}}(v)} b_e \hat{u}_v^\circ(t) n_e(v) = \sum_{e\in\mathcal{E}^{\mathrm{in}}(v)} b_e u_e^\circ(v,t) n_e(v), \qquad v \in \mathcal{V}_0 \cup \mathcal{V}_\partial^{\mathrm{out}},\ t > 0. \tag{14}$$

Condition (13) fixes the densities at the inflow vertices of the pipes $e \in \mathcal{E}^{\mathrm{out}}(v)$ to the vertex value $\hat{u}_v^\circ$, which is determined by the mixing rule (14) as a convex combination of the values $u_e^\circ(v)$ coming from the edges $e \in \mathcal{E}^{\mathrm{in}}(v)$ pointing into the vertex v. In summary, this makes up $|\mathcal{E}^{\mathrm{out}}(v)| + 1$ coupling conditions which determine the values $u_e^\circ(v)$ for the edges $e \in \mathcal{E}^{\mathrm{out}}(v)$ originating from v and the vertex value $\hat{u}_v^\circ$. Let us emphasize that the number and type of coupling conditions are different from the parabolic case $\varepsilon > 0$ above, leading to additional interior layers for vanishing diffusion $\varepsilon \to 0$; see [11] and below.

2.4. Basic assumption and preliminary results

For the rest of the presentation, we make use of the following assumptions on the problem data.

Assumption 1. *Let $0 < \varepsilon \le 1$ and $0 < \underline{b} \le b_e \le \bar{b}$ for all $e \in \mathcal{E}$ as well as*

$$\sum_{e\in\mathcal{E}(v)} b_e n_e(v) = 0, \qquad v \in \mathcal{V}_0. \tag{15}$$

Furthermore, the boundary data in (8) and (12) shall satisfy $\hat{g} \in C^{m+2}(0, t_{\max}; \ell^2(\mathcal{V}_\partial))$ for some time horizon $t_{\max} > 0$, with $\partial_t^n \hat{g}(0) = 0$ for $0 \le n \le m$ and some $m \ge 0$.

The assumptions on b characterize a steady background flow which, for ease of notation, is aligned with the orientation of the edges. Condition (15) together with the coupling conditions ensures the conservation of mass at interior vertices. The boundary data are consistent with trivial initial conditions $u^\varepsilon(0) = 0$, and hence the occurrence of initial layers is avoided. For later reference, we summarize some basic results about the solvability and regularity of solutions for our two model problems.

Lemma 2. *Let Assumption 1 hold. Then for any $\varepsilon > 0$, the convection–diffusion problem (7)–(10) has a unique solution $(u^\varepsilon, \hat{u}^\varepsilon)$ with initial value $u^\varepsilon(0) = 0$, and*

$$u^\varepsilon \in C^{m+1}\big(L^2(\mathcal{E})\big) \cap C^0\big(H_{pw}^{2m+2}(\mathcal{E}) \cap H^1(\mathcal{E})\big), \qquad \hat{u}^\varepsilon \in C^m(\ell_2(\mathcal{V}_0)), \tag{16}$$

and the derivatives of u^ε are bounded by

$$\big|\partial_t^n \partial_x^j u_e^\varepsilon(x,t)\big| \le C\left(1 + \varepsilon^{-j} e^{-b_e(\ell_e - x)/\varepsilon}\right) \tag{17}$$

for all $x \in [0, \ell_e]$, $e \in \mathcal{E}$, $0 \le t \le t_{\max}$ and $n \le m$, $j \le 2(m-n)+1$. Furthermore, also the transport problem (11)–(14) has a unique solution with initial value $u^\circ(0) = 0$, and

$$u^\circ \in C^{m+1}\big(L^2(\mathcal{E})\big) \cap C^0\big(H_{pw}^{m+1}(\mathcal{E})\big), \qquad \hat{u}^\circ \in C^m(\ell_2(\mathcal{V}_0)), \tag{18}$$

and the asymptotic estimate

$$\|u^\varepsilon - u^\circ\|_{L^\infty(0,t_{\max};L^2(\mathcal{E}))} \le C'\sqrt{\varepsilon} \tag{19}$$

holds true. The constants C, C' only depend on the bounds in Assumption 1. Here $C^m(X) = C^m([0; t_{\max}]; X)$ is the space of smooth functions on $[0, t_{\max}]$ with values in X, and $t_{\max} > 0$ the chosen time horizon.

Existence, uniqueness, and regularity of the solutions follow readily by semi-group theory; see [11, 21] and [8, 10] for details. The asymptotic estimate (19) was proven in [11]. The bounds for the derivatives can be established with similar arguments as in [19, 24, 31]. For the convenience of the reader, a detailed proof of (17) for the problem on networks is presented in Appendix A.1.

3. The hybrid discontinuous Galerkin method

We now turn to the discretization of the problems introduced in the previous section. In our analysis, we will only consider the semi-discretization in space. In combination with appropriate time-stepping schemes, all results also carry over to fully discrete approximations. Corresponding remarks and numerical tests will be presented in Section 5.

3.1. Mesh and approximation spaces

We split every edge $e \simeq (0, \ell_e)$ into appropriate sub-intervals. The global mesh is then given by

$$\mathcal{T}_h = \big\{T_e^i = \big(x_e^{i-1}, x_e^i\big) : i = 1, \dots, M_e,\ e \in \mathcal{E}\big\},$$

with $0 = x_e^0 < x_e^1 < \dots < x_e^{M_e} = \ell_e$ denoting the mesh points on the edge e. We write $h_e^i = x_e^i - x_e^{i-1}$ and $h = \max_{e,i} h_e^i$ for the local and global mesh size, and also use h_T for the size of an element $T \in \mathcal{T}_h$ below. The extremal points x_e^0 and $x_e^{M_e}$ on every edge are identified with vertices $v \in \mathcal{V}$ of the graph $\mathcal{G} = (\mathcal{V}, \mathcal{E})$, and we denote by

$$\mathcal{X}_h = \big\{x_e^i : 0 < i < M_e,\ e \in \mathcal{E}\big\}$$

the remaining mesh points in the interior of the edges. Note that the mesh $(\mathcal{T}_h, \mathcal{X}_h)$ could also be interpreted as a refinement $\mathcal{G}_h = (\mathcal{V} \cup \mathcal{X}_h, \mathcal{T}_h)$ of the original graph $\mathcal{G} = (\mathcal{V}, \mathcal{E})$. In accordance with the notation of Section 2, we define broken Sobolev spaces

$$H^k_{pw}(\mathcal{T}_h) = \big\{w \in L^2(\mathcal{E}) : w|_T \in H^k(T) \text{ for all } T \in \mathcal{T}_h\big\}.$$

For the approximation of solutions to our two model problems, we consider the spaces

$$W_h = \big\{w_h \in L^2(\mathcal{E}) : w_h|_T \in P_k(T) \text{ for all } T \in \mathcal{T}_h\big\},$$

consisting of all piecewise polynomials of degree $\le k$ over the mesh $\mathcal{T}_h$. In addition, we will make use of the space of hybrid variables

$$\hat{W}_h = \{\hat{w}_h \in \ell_2(\mathcal{V} \cup \mathcal{X}_h) :\ \hat{w}_h(v) = 0\ \forall\, v \in \mathcal{V}_\partial\}$$

to represent the vertex values at the interior mesh points and vertices. Let us note that in comparison to the continuous problem (7)–(10) where hybrid variables only exist at interior vertices $v \in \mathcal{V}_0$, we now also introduce hybrid variables at all interior mesh points $x_e^i \in \mathcal{X}_h$ as well as at boundary vertices $v \in \mathcal{V}_\partial$. An illustration is given in Figure 2. For the convenience of notation, let us introduce the grid-dependent scalar products

$$(u, w)_{\mathcal{T}_h} = \sum_{T \in \mathcal{T}_h} (u, w)_{L^2(T)}, \qquad \langle u, w\rangle_{\partial\mathcal{T}_h} = \sum_{T_e^i \in \mathcal{T}_h} u\big(x_e^{i-1}\big)w\big(x_e^{i-1}\big) + u\big(x_e^i\big)w\big(x_e^i\big),$$

as well as the associated norms $\|w\|^2_{\mathcal{T}_h} = (w, w)_{\mathcal{T}_h}$ and $|w|^2_{\partial\mathcal{T}_h} = \langle w, w\rangle_{\partial\mathcal{T}_h}$.

3.2. The hybrid-dG method

For the numerical approximation of solutions to the convection–diffusion problem on networks (7)–(10), as well as the limiting transport problem (11)–(14), we consider the following discretization scheme.

Problem 3. *Let W_h and $\hat{W}_h$ be defined as above with polynomial degree $k \ge 1$ fixed. Find $u_h^\varepsilon \in C^1([0, t_{\max}]; W_h)$ with $u_h^\varepsilon(0) = 0$ and $\hat{u}_h^\varepsilon \in C^0([0, t_{\max}]; \hat{W}_h)$, such that*

$$(\partial_t u_h^\varepsilon(t), w_h)_{\mathcal{T}_h} + b_h(u_h^\varepsilon(t), \hat{u}_h^\varepsilon(t); w_h, \hat{w}_h) + \varepsilon d_h(u_h^\varepsilon(t), \hat{u}_h^\varepsilon(t); w_h, \hat{w}_h) = \ell_h^\varepsilon(t; w_h) \tag{20}$$

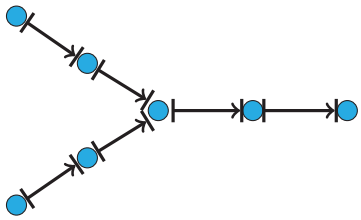

FIGURE 2. Placement of hybrid variables indicated in cyan in a simple spatial mesh with two sub-intervals per edge for the network depicted in Figure 1.

for all $w_h \in W_h$, $\hat{w}_h \in \hat{W}_h$, *and* $0 \le t \le t_{\max}$, *with bilinear and linear forms defined by*

$$b_h(u_h^\varepsilon, \hat{u}_h^\varepsilon; w_h, \hat{w}_h) = -(bu_h^\varepsilon, \partial_x w_h)_{\mathcal{T}_h} + \langle nb\, u_h^{up}, w_h - \hat{w}_h\rangle_{\partial\mathcal{T}_h}, \tag{21}$$

$$\begin{aligned} d_h(u_h^\varepsilon, \hat{u}_h^\varepsilon; w_h, \hat{w}_h) &= (\partial_x u_h^\varepsilon, \partial_x w_h)_{\mathcal{T}_h} - \langle n\partial_x u_h^\varepsilon, w_h - \hat{w}_h\rangle_{\partial\mathcal{T}_h} \\ &\quad + \langle n(u_h^\varepsilon - \hat{u}_h^\varepsilon), \partial_x w_h\rangle_{\partial\mathcal{T}_h} + \left\langle \frac{\alpha}{h_{\mathrm{loc}}}(u_h^\varepsilon - \hat{u}_h^\varepsilon), w_h - \hat{w}_h \right\rangle_{\partial\mathcal{T}_h}, \end{aligned} \tag{22}$$

$$\ell_h^\varepsilon(t; w_h) = -\langle nb\hat{g}(t), w_h\rangle_{\mathcal{V}_\partial^{\mathrm{in}}} + \langle n\varepsilon\hat{g}(t), \partial_x w_h\rangle_{\mathcal{V}_\partial} + \left\langle \frac{\alpha\varepsilon}{h_{\mathrm{loc}}}\hat{g}(t), w_h \right\rangle_{\mathcal{V}_\partial}. \tag{23}$$

Here, $nb\, u_h^{up} = \max(nb, 0)u_h^\varepsilon + \min(nb, 0)\hat{u}_h^\varepsilon$ *denotes the convective upwind flux at the vertices and interior grid points,* $h_{\mathrm{loc}}|_T = h_T$ *for* $T \in \mathcal{T}_h$, *and* $\alpha > 0$ *is a stabilization parameter for the diffusive jump terms; see [12] for a similar definition of the upwind value* u_h^{up}.

Using standard arguments, see *e.g.*, [7,32], one can obtain the following local error estimate. For convenience of the reader, a complete proof is provided in Appendix A.3.

Lemma 4. *Let Assumption 1 hold and* $(u^\varepsilon, \hat{u}^\varepsilon)$ *be the solution of* (7)–(10) *with initial value* $u^\varepsilon(0) = 0$. *Further, let* $(u_h^\varepsilon, \hat{u}_h^\varepsilon)$ *be the corresponding solution of Problem 3. Then*

$$\|u^\varepsilon(t) - u_h^\varepsilon(t)\|_{L^2(\mathcal{E})}^2 \le C \sum_{T\in\mathcal{T}_h} \left(\varepsilon h_T^{2k} + h_T^{2k+2}\right) \|u^\varepsilon\|_{H^1(0,t_{\max};H^{k+1}(T))}^2 \tag{24}$$

for all $0 < t < t_{\max}$ *with constant* C *independent of* ε *and* $\mathcal{T}_h$.

Remark 5. The above scheme falls into the class of *hybridizable dG methods* introduced in [4]. By formally setting $\varepsilon = 0$, we obtain a consistent approximation for the limiting transport problem (11)–(14), which was analyzed in [10]. The bound (24) holds verbatim for $\varepsilon = 0$ and yields order optimal estimates $\|u^\circ - u_h^\circ\|_{L^\infty(0,T;L^2(\mathcal{E}))} \le Ch^{k+1}$ for the approximation of the limiting transport problem on uniform meshes. On such meshes, however, we do not expect convergence for $\varepsilon \to 0$ due to the blow-up of the derivatives of u^ε, see Lemma 2, leading to degenerate bounds on the right-hand side of (24).

4. The main result

In order to deal with the singularities of the solution u^ε for $\varepsilon \to 0$, we consider approximations on layer-adapted grids. This will allow us to establish error estimates that are uniform in the asymptotic parameter ε.

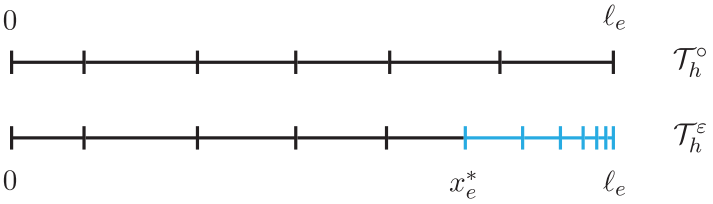

FIGURE 3. Quasi-uniform mesh $\mathcal{T}_h^\circ$ for a single pipe (*top*) and corresponding adaptive mesh $\mathcal{T}_h^\varepsilon = \mathcal{T}_h^{\varepsilon,1} \cup \mathcal{T}_h^{\varepsilon,2}$ (*bottom*). The layer region (x_e^*, ℓ^e) is depicted in cyan.

4.1. Construction of the adaptive grids

When $\varepsilon < h^{2k}$ we will use a quasi-uniform grid $\mathcal{T}_h = \mathcal{T}_h^\circ$ with mesh size $h_T \approx h$ for all elements $T \in \mathcal{T}_h$. For $\varepsilon \geq h^{2k}$ we construct a layer-adapted grid $\mathcal{T}_h^\varepsilon$ as follows: For every edge $e \in \mathcal{E}$ we define a transition point

$$x_e^* := \ell_e - \frac{k+1}{b_e}\varepsilon \log(1/\varepsilon). \tag{25}$$

On the intervals $[0, x_e^*)$ we consider the mesh-points inherited from the uniform mesh $\mathcal{T}_h^\circ$, augmented by the transition point $x_e^* =: x_e^{M_e^*}$. The corresponding elements are collected in the set $\mathcal{T}_h^{\varepsilon,1}$. By construction, we have $h_T \lesssim h$ for $T \in \mathcal{T}_h^{\varepsilon,1}$ and $|\mathcal{T}_h^{\varepsilon,1}| = M_e^* \leq Ch^{-1}$. In the layer region $(x_e^*, \ell_e]$, the mesh points are defined recursively by

$$h_e^i = \varepsilon h e^{b_e(\ell_e - x_e^i)/\varepsilon(k+1)}, \qquad x_e^{i-1} = x_e^i - h_e^i, \qquad i \leq M_e, \tag{26}$$

with $x_e^{M_e} = \ell_e$ denoting the outflow vertex of the edge $e \simeq (0, \ell_e)$. The index M_e is chosen such that $x_e^{M_e^*+1}$ is the last point in this sequence which is strictly larger than the transition point x_e^*; see Figure 3.

The elements in the layer region, generated by the points x_e^i with $M_e^* \leq i \leq M_e$, are collected in the set $\mathcal{T}_h^{\varepsilon,2}$. Using a slight modification of the arguments in [15, 28] and the condition $\varepsilon \geq h^{2k}$, one can show that $|\mathcal{T}_h^{\varepsilon,2}| \leq Ch^{-1}$ with C independent of h and ε; see Section 4.3 below. The complete layer-adapted mesh $\mathcal{T}_h^\varepsilon = \mathcal{T}_h^{\varepsilon,1} \cup \mathcal{T}_h^{\varepsilon,2}$ is then simply obtained by accumulation.

4.2. Uniform error estimate

We can now fully describe our adaptive approximation scheme and state the main result of this paper.

Theorem 6. *Let Assumption 1 hold, and let $(u^\varepsilon, \hat{u}^\varepsilon)$ be the unique solution of the convection-diffusion problem (7)–(10) with initial value $u^\varepsilon(0) = 0$. Further, define*

$$\tilde{u}_h^\varepsilon := \begin{cases} u_h^\circ, & \text{if } \varepsilon < h^{2k}, \\ u_h^\varepsilon, & \text{if } \varepsilon \geq h^{2k}, \end{cases}$$

where $(u_h^\circ, \hat{u}_h^\circ)$ is the solution of Problem 3 with $\varepsilon = 0$ on the mesh $\mathcal{T}_h = \mathcal{T}_h^\circ$, while $(u_h^\varepsilon, \hat{u}_h^\varepsilon)$ is the solution of Problem 3 on the layer-adapted mesh $\mathcal{T}_h = \mathcal{T}_h^\varepsilon$. Then

$$\|u^\varepsilon - \tilde{u}_h^\varepsilon\|_{L^\infty(0,t_{\max};L^2(\mathcal{E}))} \leq C \max\big(h^{k+1}, \min\big(\sqrt{\varepsilon}, h^k\big)\big). \tag{27}$$

Moreover, the number of elements in $\mathcal{T}_h^\varepsilon$ can be bounded by $C'h^{-1}$. The constants C, C' in these estimates only depend on the bounds in Assumption 1, but not on ε or h.

Remark 7. Since the number of elements $N = |\mathcal{T}_h^\varepsilon| \approx C' h^{-1}$, we immediately obtain corresponding bounds

$$\|u^\varepsilon - \tilde{u}_h^\varepsilon\|_{L^\infty(0,t_{\max};L^2(\mathcal{E}))} \le C'' \max\bigl(N^{-k-1}, \min\bigl(\sqrt{\varepsilon}, N^{-k}\bigr)\bigr).$$

A quick look into the error analysis reveals, that one can derive corresponding bounds for the error $\|u^\varepsilon - \tilde{u}_h^\varepsilon\|_{\varepsilon,h}$ in the mesh- and parameter dependent dG-norm; see [7,28,32]. By formally setting $\varepsilon = 0$, we obtain the error estimate for the hybrid-dG approximation of the pure transport problem on a quasi-uniform grid, which was established in [10].

4.3. Proof of Theorem 6

The two cases which are exploited in the construction of the adaptive approximation scheme are treated separately in the following. Note that all constants appearing here and in subsequent proofs only depend on the bounds in Assumption 1, but not on ε or h.

Case 1: $\varepsilon < h^{2k}$. By construction, we have $\tilde{u}_h^\varepsilon = u_h^\circ$, where u_h° denotes the hybrid-dG approximation of the transport problem. Using the triangle inequality, we obtain

$$\begin{aligned}\|u^\varepsilon - \tilde{u}_h^\varepsilon\|_{L^\infty(0,t_{\max};L^2(\mathcal{E}))} &= \|u^\varepsilon - u_h^\circ\|_{L^\infty(0,t_{\max};L^2(\mathcal{E}))}\\ &\le \|u^\varepsilon - u^\circ\|_{L^\infty(0,t_{\max};L^2(\mathcal{E}))} + \|u^\circ - u_h^\circ\|_{L^\infty(0,t_{\max};L^2(\mathcal{E}))}\\ &\le c\sqrt{\varepsilon} + c' h^{k+1} \le C \max\bigl(\sqrt{\varepsilon}, h^{k+1}\bigr),\end{aligned}$$

with $(u^\circ, \hat{u}^\circ)$ being the solution of (11)–(14). Here, we employed the asymptotic estimate (19) for the continuous solution as well as the error estimate for the hybrid-dG approximation of the limiting transport problem; see [10]. This already yields the bound (27) for the case $\varepsilon < h^{2k}$. The assertion about the number of elements is clear since the mesh $\mathcal{T}_h = \mathcal{T}_h^\circ$ is quasi-uniform.

Case 2: $\varepsilon \ge h^{2k}$. From Lemma 4, we already know that

$$\|u^\varepsilon(t) - u_h^\varepsilon(t)\|_{L^2(\mathcal{E})}^2 \le c \sum_{T\in\mathcal{T}_h^\varepsilon} \bigl(\varepsilon h_T^{2k} + h_T^{2k+2}\bigr) \|u^\varepsilon\|_{H^1(0,t_{\max};H^{k+1}(T))}^2. \tag{28}$$

Using the bounds (17), the choice of the transition point x_e^*, and noting that $h_T \approx h$ is uniform for elements $T \in \mathcal{T}_h^{\varepsilon,1}$, we find that

$$\sum_{T\in\mathcal{T}_h^1} \bigl(\varepsilon h_T^{2k} + h_T^{2k+2}\bigr) \|u^\varepsilon\|_{H^1(0,t_{\max};H^{k+1}(T))}^2 \le c' \bigl(\varepsilon h^{2k} + h^{2k+2}\bigr) \le 2c' h^{2k}.$$

In the layer-adapted part $\mathcal{T}_h^{\varepsilon,2}$ of the mesh, the local mesh sizes h_e^i are determined recursively by (26), and the bounds (17) allow us to estimate

$$\begin{aligned}&\sum_{T_e^i\in\mathcal{T}_h^{\varepsilon,2}} \Bigl(\varepsilon \bigl(h_e^i\bigr)^{2k} + \bigl(h_e^i\bigr)^{2k+2}\Bigr) \|u^\varepsilon\|_{H^1(0,t_{\max};H^{k+1}(T_e^i))}^2\\ &\qquad \le c' \sum_{T_e^i\in\mathcal{T}_h^{\varepsilon,2}} \Bigl(\varepsilon \bigl(h_e^i\bigr)^{2k} + \bigl(h_e^i\bigr)^{2k+2}\Bigr) \int_{x_e^{i-1}}^{x_e^i} \varepsilon^{-2k-2} e^{-2b_e(\ell_e - x)/\varepsilon}\,\mathrm{d}x =: \text{(i)} + \text{(ii)}.\end{aligned}$$

Using the choice $h_e^i = \varepsilon h e^{b_e(\ell_e - x_e^i)/\varepsilon(k+1)}$ in (26), the first term can be estimated by

$$\text{(i)} \le c' \sum_{T_e^i \in \mathcal{T}_h^{\varepsilon,2}} \varepsilon^{-1} h^{2k} \int_{x_e^{i-1}}^{x_e^i} e^{2kb_e(\ell_e - x)/(k+1)} e^{-2b_e(\ell_e - x)/\varepsilon} \,\mathrm{d}x$$
$$= c' \sum_{e \in \mathcal{E}} \varepsilon^{-1} h^{2k} \int_{x_e^*}^{\ell_e} e^{-2b_e(\ell_e - x)/\varepsilon(k+1)} \,\mathrm{d}x \le c'' h^{2k},$$

since the pipe network is finite. Similarly, we obtain for the second term

$$\text{(ii)} \le c' h^{2k+2} \sum_{T_e^i \in \mathcal{T}_h^{\varepsilon,2}} h_e^i \le c' h^{2k+2} \sum_{e \in \mathcal{E}} (\ell_e - x_e^*) \le c'' h^{2k+2}.$$

Adding the two estimates for $\mathcal{T}_h^{\varepsilon,1}$ and $\mathcal{T}_h^{\varepsilon,2}$ yields the bound (27) for $\varepsilon \ge h^{2k}$.

It remains to verify the bound on the number of elements: The graded mesh $\mathcal{T}_h^{\varepsilon,2}$ is of Gartland-type, and using the arguments employed in [15], p. 645 and [28], p. 8, one can see that the number of elements in $\mathcal{T}_h^{\varepsilon,2}$ intersecting the intervals (x_e^S, ℓ_e), with $x_e^S = \ell_e - \frac{k+1}{b_e}\varepsilon \log(1/h)$ denoting the Shishkin transition point, is bounded by $c' h^{-1}$. By assumption, we further have $\varepsilon \ge h^{2k}$, and therefore $|\ell_e - x_e^*| \le 2k|\ell - x_e^S|$. Since the mesh gets coarser when moving away from the layer, we conclude that $|\mathcal{T}_h^\varepsilon| \le C' h^{-1}$ with $C' \le 2kc'$. By a refined analysis, this estimate could even be further improved, *i.e.*, the number of elements intersecting the region (x_e^*, x_e^S) is bounded by $c'' \log(1/h)$, which would yield $C' \le c' + c'' \log(1/h) h^{-1}$. This completes the proof. □

5. Numerical tests

In order to illustrate the flexibility and performance of the proposed hybrid-dG scheme, we now present some numerical results. We first discuss in detail the convergence behavior for a problem on a single pipe, and then briefly discuss a test problem on a pipe network.

5.1. Single pipe

We consider a single pipe $e = (v_1, v_2) \simeq (0, 1)$ of length $\ell = 1$. The flow velocity is chosen as $b = 1$, and the boundary conditions are described by

$$\hat{g}_{v_1}(t) = \frac{1}{t_{\max}} t^3, \qquad \hat{g}_{v_2} = 0.$$

The simulations are performed for time $t \le t_{\max} = 3$, and the initial conditions are given by $u^\varepsilon(0) = 0$. This choice of the problem data satisfies Assumption 1 with $m = 2$, which suffices to guarantee optimal convergence rates for polynomial order $k \le 2$.

Discretization and error estimation. For our numerical tests, we utilize the proposed hybrid-dG method with piecewise quadratic finite elements, and we set $\alpha = 1$ for the stabilization parameter. The convergence rates of Theorem 6 apply with $k = 2$. For the time integration, we use the Radau IIA Runge–Kutta method with 3 stages and a uniform time step τ. This scheme can be interpreted as a discontinuous Galerkin method with second-order polynomials, and the time-discretization errors can be shown to be of order $O(\tau^3)$; see [1,32]. We choose $\tau = h/2$, such that the effect of the time discretization can be considered negligible. To estimate the discretization errors, we compute a reference solution $u_{\mathrm{ref}}^\varepsilon$ on a mesh $\mathcal{T}_h^{\mathrm{ref}}$, which is obtained by two uniform refinements of the computational mesh $\mathcal{T}_h$ used in our analysis. In addition, the time step $\tau^{\mathrm{ref}} = \tau/4$ is reduced accordingly. The actual discretization error is then estimated by

$$\|u^\varepsilon - \tilde{u}_h^\varepsilon\|_{\mathrm{ref}} := \max_{n=0,\dots,N_{\mathrm{ref}}} \|(u_{\mathrm{ref}}^\varepsilon)(t^n) - (I_{\mathrm{ref}} \tilde{u}_h^\varepsilon)(t^n)\|_{L^2(\mathcal{E})}, \tag{29}$$

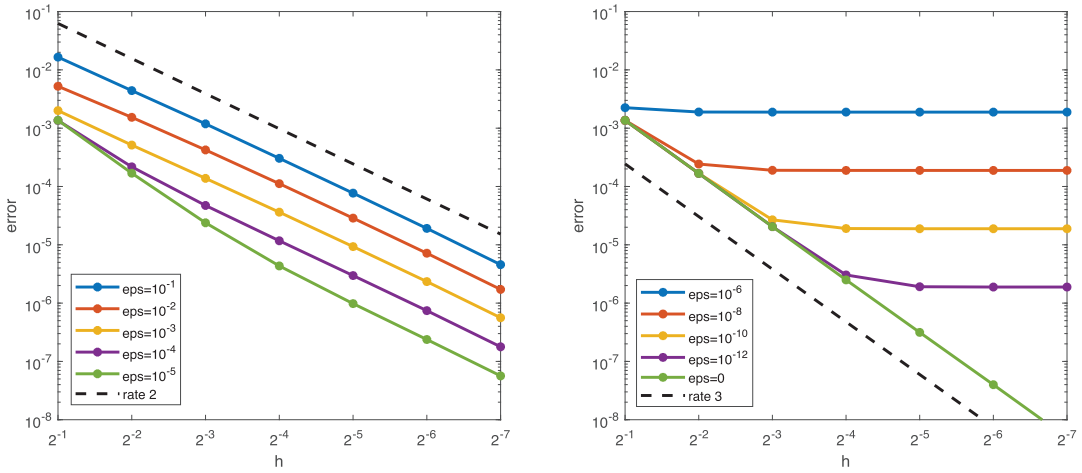

FIGURE 4. *Left*: Error for $\tilde{u}_h^\varepsilon = u_h^\varepsilon$ on graded mesh $\mathcal{T}_h^\varepsilon$. *Right*: Error for $\tilde{u}_h^\varepsilon = u_h^\circ$ on $\mathcal{T}_h^\circ$.

where I_{ref} denotes the interpolation operator onto the reference mesh and N_{ref} is the number of time steps used for the computation of the reference solution.

Results. In the left plot of Figure 4, we display the numerical errors $\|u^\varepsilon - \tilde{u}_h^\varepsilon\|_{\mathrm{ref}}$ obtained by the hybrid-dG method on the graded mesh $\mathcal{T}_h^\varepsilon$ for different values of $\varepsilon > 0$. This is the relevant error in the diffusive regime $\varepsilon \geq h^{2k}$. In accordance with Theorem 6, we observe second-order convergence. On coarse meshes and for small ε, the diffusive terms can be considered as a perturbation of the pure transport problem, which explains the increase in the convergence rate for the test with $\varepsilon = 10^{-5}$. In our tests, the number of elements $|\mathcal{T}_h^{\varepsilon,2}|$ in the boundary layer (x^*, ℓ) is approximately $3 \cdot h^{-1}$, and only few elements lie in the layer (x^*, x^S) outside the Shishkin point; see Section 4.3. In the right part of Figure 4, we plot the errors $\|u^\varepsilon - u_h^\circ\|_{\mathrm{ref}}$, which are relevant when $\varepsilon < h^{2k}$. From the proof of Theorem 6, one can see that $\|u^\varepsilon - u_h^\circ\|_{\mathrm{ref}} \leq c\sqrt{\varepsilon} + c' h^{k+1}$. This leads to a saturation when $c\sqrt{\varepsilon} \approx c' h^{k+1}$, *i.e.*, $\sqrt{\varepsilon}$ becomes the dominating term in the error estimate. However, the saturation is already occurring a bit earlier on a coarser mesh, since the dominating effect of $\sqrt{\varepsilon}$ starts to show up. In summary, the numerical results are in perfect agreement with the theoretical predictions.

5.2. A pipe network

As a second test problem, we consider a pipe network consisting of 11 edges and 11 vertices, with 3 entries, 2 exits and 1 loop; see Figure 5 for a sketch. For ease of presentation, we set $\ell_e = 1$ for the length of all edges. The volume flow rates are given by

$$b_{e_1} = b_{e_2} = b_{e_5} = b_{e_6} = b_{e_9} = 2, \quad b_{e_3} = b_{e_8} = b_{e_{10}} = b_{e_{11}} = 1, \quad b_{e_4} = b_{e_7} = 3.$$

By this choice, condition (15) is satisfied. As boundary conditions we choose

$$\hat{g}_{v_1}(t) = \frac{2}{t_{\max}^3} t^3, \quad \hat{g}_{v_4}(t) = \hat{g}_{v_7}(t) = 0, \quad \hat{g}_{v_{10}}(t) = \frac{3}{2t_{\max}^4} t^4, \quad \hat{g}_{v_{11}}(t) = \frac{5}{2t_{\max}^3} t^3.$$

The time horizon is set to $t_{\max} = 6$, and the initial conditions are again $u^\varepsilon(0) = u^\circ(0) = 0$. Like in the previous test, Assumption 1 is satisfied with the smoothness parameter $m = 2$.

Results. At the vertices v_3, v_8, and v_9, which have two in-going and one out-going pipe, we expect discontinuities in the concentration field in the transport limit $\varepsilon = 0$, and corresponding internal layers for the

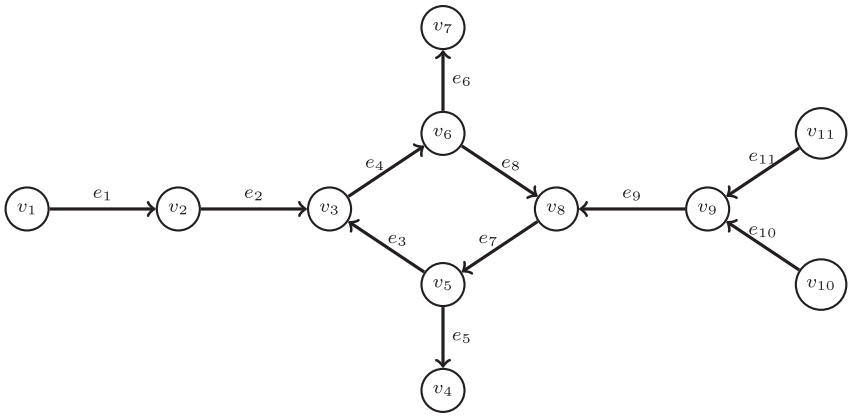

FIGURE 5. Topology of the GasLib-11 network, taken from [29].

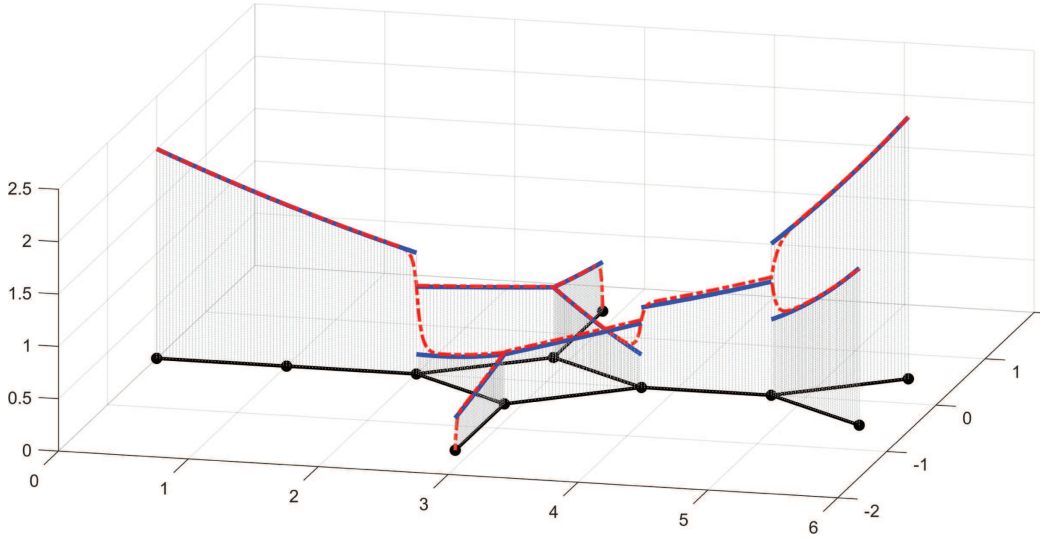

FIGURE 6. Solution to the convection-diffusion problem for $\varepsilon = 0.05$ (red, dashed) and the limiting transport problem for $\varepsilon = 0$ (blue, solid). Discontinuities appearing for the transport limit are smoothed out for $\varepsilon > 0$ by diffusion, leading to boundary layers at the outflow boundaries and internal junctions. Away from the layers, the solutions to the two different problems can hardly be distinguished.

convection–diffusion problem with $\varepsilon > 0$. Furthermore, we expect boundary layers at the outflow vertices v_4 and v_7; compare with the plot in Figure 6. Using the same discretization strategy and test setup as explained for the case of a single pipe, we repeated the convergence tests and observed exactly the same convergence behavior as depicted in Figure 4 for the case of a single pipe. Since no additional insight is obtained from these results, we omit their presentation here.

6. Discussion

In this paper, we studied the numerical approximation of singularly perturbed parabolic convection-diffusion problems on one-dimensional pipe networks by a hybrid discontinuous Galerkin method. A key feature of this method is the correct handling of the coupling conditions at network junctions and boundary conditions at network boundaries, whose number and type changes in the vanishing diffusion limit $\varepsilon \to 0$. To avoid possible instabilities resulting from the boundary and internal layers, geometrically adapted meshes of Gartland-type were employed in the layer regions.

In the transport regime, *i.e.*, when $\varepsilon < h^{2k}$, we proposed to use the numerical approximation of the pure transport problem. This allowed us to choose the transition point for the layer adapted mesh as $x^*(\varepsilon) \approx \ell - \varepsilon \log(1/\varepsilon)$, while still guaranteeing a quasi-optimal number $N \approx h^{-1}$ of elements. Moreover, this choice allowed us to resort to standard localized discretization error estimates for dG methods. The numerical results demonstrate the validity and sharpness of our estimates.

For lowest order approximations with $k = 1$, we observed convergence of order $O(h^{k+1})$ even in the diffusion-dominated regime. While the use of hybrid variables in our discretization method is particularly useful for the automatic handling of the coupling conditions at network junctions, alternative discretization strategies, *e.g.*, standard dG schemes, upwind finite differences, or SUPG-Galerkin methods, may be used for the approximation along the pipes. The main steps of our analysis should carry over to such schemes almost verbatim. Also, the additional consideration of time discretization seems possible without major complications. A theoretical investigation of these topics is left for future research.

Appendix A.

For completeness of the presentation, we now give the proofs for some auxiliary results, which were used in our error analysis and follow by standard arguments.

A.1. Proof of the bounds (17) in Lemma 2

Let u^ε be the solution of (7)–(10) with initial value $u^\varepsilon(0) = 0$. We want to show that

$$\left|\partial_t^n \partial_x^j u_e^\varepsilon(x,t)\right| \le C\left(1 + \varepsilon^{-j} e^{-b_e(\ell_e - x)/\varepsilon}\right) \tag{A.1}$$

for all $n \le m$, $j \le 2(m-n)+1$; recall that m is the regularity index of Assumption 1. For establishing these bounds, we will use the following weak maximum principle for convection-diffusion problems on networks; see Lemma 7 of [11].

Lemma A.1. *Let $u \in C^1([0,t_{\max}]; L^2(\mathcal{E})) \cap C^0([0,t_{\max}]; H^1(\mathcal{E}) \cap H^2_{pw}(\mathcal{E}))$ satisfy*

$$\begin{aligned} \partial_t u_e + b_e \partial_x u_e - \varepsilon \partial_{xx} u_e &\ge 0, && \forall e \in \mathcal{E}, \\ \sum_{e \in \mathcal{E}(v)} \varepsilon \partial_x u_e(v) n_e(v) &= 0, && \forall v \in \mathcal{V}_0, \\ u(v) &\ge 0, && \forall v \in \mathcal{V}_\partial, \end{aligned}$$

for all $0 < t < t_{\max}$ with initial conditions

$$u(0) \ge 0, \qquad \forall e \in \mathcal{E}.$$

Then, the function u is non-negative, i.e., $u \ge 0$ on $\mathcal{E}$ for all $t \in [0,t_{\max}]$.

The above estimates can now be established by induction over j and n. For $j, n = 0$ the claim follows directly from Lemma A.1 with the usual comparison arguments: We define $w_e(x,t) := \max_t |\hat{g}(t)| \pm u_e^\varepsilon(x,t)$, which satisfies all conditions of Lemma A.1, and therefore is non-negative. This implies that $|u^\varepsilon|$ can be bounded by the maximum norm of the boundary data $\hat{g}$. By linearity and time-invariance of the equations, $(\partial_t^n u^\varepsilon, \partial_t^n \hat{u}^\varepsilon)$ again solves (7)–(10), but with boundary data $\partial_t^n \hat{g}$; further note that $\partial_t^n u^\varepsilon(0) = 0$ for $n \le m$. With the same reasoning as above we thus obtain the bounds for $|\partial_t^n u^\varepsilon|$, $n \le m$.

Induction over j: Assume that (A.1) holds for all $0 \le i \le j-1$ and all $n \le m$. In a first step, we verify that $\partial_t^n \partial_x^j u_e^\varepsilon(\ell_e) \le c\,\varepsilon^{-j}$ for all $e \in \mathcal{E}$. By the mean value theorem, we know that there exists $y \in (\ell_e - \varepsilon, \ell_e)$, such that

$$\partial_t^n \partial_x^j u_e^\varepsilon(y) = \frac{1}{\varepsilon}\big(\partial_t^n \partial_x^{j-1} u_e^\varepsilon(\ell_e) - \partial_t^n \partial_x^{j-1} u_e^\varepsilon(\ell_e - \varepsilon)\big) \le c\,\varepsilon^{-j},$$

where we used the induction hypothesis in the last step. Using (7), we further see that

$$\partial_t\big(\partial_t^n \partial_x^j u_e^\varepsilon\big) = -b_e \partial_x\big(\partial_t^n \partial_x^j u_e^\varepsilon\big) + \varepsilon \partial_{xx}\big(\partial_t^n \partial_x^j u_e^\varepsilon\big). \tag{A.2}$$

By the fundamental theorem of calculus and the induction hypothesis, we conclude that

$$\begin{aligned}
\partial_t^n \partial_x^j u_e^\varepsilon(\ell_e) &= \partial_t^n \partial_x^j u_e^\varepsilon(y) + \int_y^{\ell_e} \partial_{xx} \partial_t^n \partial_x^{j-1} u_e^\varepsilon(x)\,\mathrm{d}x \\
&= \partial_t^n \partial_x^j u_e^\varepsilon(y) + \int_y^{\ell_e} \frac{1}{\varepsilon}\big(\partial_t^{n+1} \partial_x^{j-1} u_e^\varepsilon(x) + b_e \partial_t^n \partial_x^j u_e^\varepsilon(x)\big)\,\mathrm{d}x \\
&\le c\,\varepsilon^{-j} + \max_{x \in [y,\ell_e]} \left(\big|\partial_t^{n+1} \partial_x^{j-1} u_e^\varepsilon(x)\big| + \frac{2}{\varepsilon} b_e \partial_t^n \partial_x^{j-1} u_e^\varepsilon(x)| \right) \le c'\varepsilon^{-j}.
\end{aligned} \tag{A.3}$$

Let us now fix an arbitrary $t \in [0, t_{\max}]$ and set $w(x) := \partial_t^n \partial_x^j u^\varepsilon(x,t)$. Then by (A.2), the function w solves the ordinary differential equation

$$b_e w(x) - \varepsilon w'(x) = \eta(x) := -\partial_t^{n+1} \partial_x^{j-1} u_e^\varepsilon(x,t) \tag{A.4}$$

with terminal value $w(\ell_e) = \partial_t^n \partial_x^j u^\varepsilon(\ell_e, t)$. Using the induction hypothesis, the right hand side of this problem can be estimated by

$$|\eta(x)| \le c\Big(1 + \varepsilon^{-(j-1)} e^{-b_e(\ell_e - x)/\varepsilon}\Big). \tag{A.5}$$

Expressing the solution of (A.4) *via* the variation-of-constants-formula, we find that

$$\begin{aligned}
w(x) &= w(\ell_e) e^{-b_e(\ell_e - x)/\varepsilon} + \frac{1}{\varepsilon} \int_x^{\ell_e} e^{-b_e(\sigma - x)/\varepsilon} \eta(\sigma)\,\mathrm{d}\sigma \\
&\le c'\,\varepsilon^{-j} e^{-b_e(\ell_e - x)/\varepsilon} + \frac{1}{\varepsilon} \int_x^{\ell_e} e^{-b_e(\sigma - x)/\varepsilon} c\Big(1 + \varepsilon^{-(j-1)} e^{-b_e(\ell_e - \sigma)/\varepsilon}\Big)\,\mathrm{d}\sigma \\
&\le c'\,\varepsilon^{-j} e^{-b_e(\ell_e - x)/\varepsilon} + c\varepsilon^{-j} e^{-b_e(\ell_e - x)/\varepsilon}(\ell - x) + \frac{c}{b_e}\Big(1 - e^{-b_e(\ell - x)/\varepsilon}\Big) \\
&\le c\Big(1 + \varepsilon^{-j} e^{-b_e(\ell_e - x)/\varepsilon}\Big).
\end{aligned}$$

Here we employed (A.3) and (A.5) in the subsequent estimates. This yields the bounds (17) for index $i = j$ and $n \le m$ and, by induction, concludes the proof of Lemma 2. □

A.2. Basic properties of the hybrid-dG scheme

We now establish discrete stability, well-posedness, and consistency of the discretization scheme in Problem 3. We start with showing ellipticity of the governing bilinear forms.

Lemma A.2. *Let b_h, d_h be as in (21) and (22). Then for all $w_h \in W_h$ and $\hat{w}_h \in \hat{W}_h$, we have*

$$b_h(w_h, \hat{w}_h; w_h, \hat{w}_h) = \frac{1}{2}\left|b^{1/2}(w_h - \hat{w}_h)\right|^2_{\partial\mathcal{T}_h}, \tag{A.6}$$

$$d_h(w_h, \hat{w}_h; w_h, \hat{w}_h) = \left\|\partial_x w_h^2\right\|^2_{\mathcal{T}_h} + \left|\left(\frac{\alpha}{h_{\mathrm{loc}}}\right)^{1/2}(w_h - \hat{w}_h)\right|^2_{\partial\mathcal{T}_h} \tag{A.7}$$

with $h_{\mathrm{loc}}|_T = h_T$ for $T \in \mathcal{T}_h$.

Proof. Let $T = (x^{\mathrm{in}}, x^{\mathrm{out}})$ be one of the elements of the mesh $\mathcal{T}_h$. Then, in accordance with the notation introduced in Section 2.1, we call x^{in} the inflow and x^{out} the outflow boundary of T, and we denote by $\partial\mathcal{T}_h^{\mathrm{in}}$ and $\partial\mathcal{T}_h^{\mathrm{out}}$ the collections of all inflow and outflow boundaries of elements $T \in \mathcal{T}_h$. Equation (A.6) then follows from

$$\begin{aligned} b_h(w_h, \hat{w}_h, w_h, \hat{w}_h) &= -(b\, w_h, \partial_x w_h)_{\mathcal{T}_h} + \langle nb\, w_h^{up}, w_h - \hat{w}_h\rangle_{\partial\mathcal{T}_h} \\ &= -\frac{1}{2}\langle nb\, w_h, w_h\rangle_{\partial\mathcal{T}_h} + \langle nb\, w_h, w_h - \hat{w}_h\rangle_{\partial\mathcal{T}_h^{\mathrm{out}}} + \langle nb\, \hat{w}_h, w_h - \hat{w}_h\rangle_{\partial\mathcal{T}_h^{\mathrm{in}}} \\ &= \frac{1}{2}\left|b^{1/2} w_h\right|^2_{\partial\mathcal{T}_h} - \langle b\, w_h, \hat{w}_h\rangle_{\partial\mathcal{T}_h} + \frac{1}{2}\left|b^{1/2}\hat{w}_h\right|^2_{\partial\mathcal{T}_h} = \frac{1}{2}\left|b^{1/2}(w_h - \hat{w}_h)\right|^2_{\partial\mathcal{T}_h}. \end{aligned}$$

Here we used that $|b^{1/2}\hat{w}_h|_{\partial\mathcal{T}_h^{\mathrm{in}}} = |b^{1/2}\hat{w}_h|_{\partial\mathcal{T}_h^{\mathrm{out}}}$ due to the conservation condition (15) on the flow rates, and the fact that $\hat{w}_h(v) = 0$ for $v \in \mathcal{V}_\partial$. Equation (A.7), on the other hand, follows directly, since the second and third term in (22) cancel each other. □

As a direct consequence, we obtain the well-posedness of the discretization scheme.

Lemma A.3. *Let Assumption 1 hold. Then Problem 3 has a unique solution*

$$(u_h^\varepsilon, \hat{u}_h^\varepsilon) \in C^1([0, t_{\max}]; W_h) \times C^0([0, t_{\max}]; \hat{W}_h).$$

Proof. From the previous lemma, we can deduce that the combined bilinear form $b_h + \varepsilon d_h$ is elliptic on the discrete spaces $W_h \times \hat{W}_h$. The hybrid variables $\hat{u}_h^\varepsilon$ can therefore be eliminated from the discrete problem on the algebraic level, leading to an ordinary differential equation for u_h^ε alone. Existence of a unique solution and its regularity then follow by the Picard–Lindelöf theorem and elementary arguments. □

As a next ingredient for our analysis, we verify consistency of the approximation scheme.

Lemma A.4. *Let $(u^\varepsilon, \hat{u}^\varepsilon)$ be the solution of (7)–(10) with initial value $u^\varepsilon(0) = 0$. Further define $\hat{u}^\varepsilon(x) = u^\varepsilon(x)$ for $x \in \mathcal{X}_h$ and set $\hat{u}^\varepsilon(v) = 0$ for $v \in \mathcal{V}_\partial$. Then*

$$(\partial_t u^\varepsilon(t), w_h)_{\mathcal{T}_h} + b_h(u^\varepsilon(t), \hat{u}^\varepsilon(t); w_h, \hat{w}_h) + \varepsilon d_h(u^\varepsilon(t), \hat{u}^\varepsilon(t); w_h, \hat{w}_h) = \ell_h^\varepsilon(t; w_h)$$

for all $w_h \in W_h$, $\hat{w}_h \in \hat{W}_h$, and all $0 \le t \le t_{\max}$, i.e., the method is consistent.

Proof. Let us first test the bilinear form d_h with $w_h \in W_h$ and $\hat{w}_h \equiv 0$, which yields

$$d_h(u^\varepsilon, \hat{u}^\varepsilon; w_h, 0) = (\partial_x u^\varepsilon, \partial_x w_h)_{\mathcal{T}_h} - \langle n\partial_x u^\varepsilon, w_h\rangle_{\partial\mathcal{T}_h} + \langle n(u^\varepsilon - \hat{u}^\varepsilon), \partial_x w_h\rangle_{\partial\mathcal{T}_h} + \left\langle \frac{\alpha}{h_{\rm loc}}(u^\varepsilon - \hat{u}_\varepsilon), w_h \right\rangle_{\partial\mathcal{T}_h}$$
$$= -(\partial_{xx} u^\varepsilon, \partial_x w_h)_{\mathcal{T}_h} + \langle nu^\varepsilon, \partial_x w_h\rangle_{\mathcal{V}_\partial} + \left\langle \frac{\alpha}{h_{\rm loc}} u^\varepsilon, w_h \right\rangle_{\mathcal{V}_\partial}.$$

Here we used integration-by-parts on every element for the first term, whose boundary contributions cancels the second term. Since $u^\varepsilon(x) = \hat{u}^\varepsilon(x)$ for all $x \in \mathcal{X}_h \cup \mathcal{V}_0$, the contributions of the third and fourth term vanish at internal mesh points; further note that $\hat{u}^\varepsilon(v) = 0$ on the network boundary $v \in \mathcal{V}_\partial$. In a similar manner, we observe that

$$b_h(u^\varepsilon, \hat{u}^\varepsilon; w_h, 0) = -(b\,u^\varepsilon, \partial_x w_h)_{\mathcal{T}_h} + \langle bn\,u^{up}, w_h\rangle_{\partial\mathcal{T}_h} = (b\partial_x u^\varepsilon, w_h)_{\mathcal{T}_h}$$

for all $w_h \in W_h$, since $nb\,u^{up}(v) := \max(nb,0)u^\varepsilon(v) + \min(nb,0)\hat{u}^\varepsilon(v) = nb\,u^\varepsilon(v) - nb\,\hat{g}(v)|_{\mathcal{V}_\partial^{\rm in}}$ by continuity of u^ε across junctions and due to the fact that $\hat{u}^\varepsilon(v) = 0$ at $\mathcal{V}_\partial$. Using (7) and (8), we then see that

$$(\partial_t u_h^\varepsilon, w_h)_{\mathcal{T}_h} + b_h(u_h^\varepsilon, \hat{u}_h^\varepsilon; w_h, 0) + \varepsilon d_h(u_h^\varepsilon, \hat{u}_h^\varepsilon; w_h, 0) = \ell_h(w_h)$$

for all $w_h \in W_h$ and $0 \le t \le t_{\max}$. The continuity and coupling conditions (9) and (10), on the other hand, imply validity of the variational identities for $\hat{w}_h \in \hat{W}_h$ when testing with $w_h \equiv 0$. In summary, we thus obtain consistency of the method. □

A.3. Proof of Lemma 4

Based on consistency and discrete stability, we can now prove the local error estimate (24). Following ([32], Chap. 12), we define a projection operator $\pi_h : H^1_{pw}(\mathcal{E}) \to W_h$ by

$$\pi_h w^-\big(x_e^i\big) = w^-\big(x_e^i\big) \quad \text{for all } i = 1, \dots, M_e,\ e \in \mathcal{E}, \tag{A.8}$$
$$\int_T (w - \pi_h w) p \,\mathrm{d}x = 0 \qquad \text{for all } p \in P_{k-1}(T),\ T \in \mathcal{T}_h \tag{A.9}$$

with up- and downwind value of w at some point x denoted by

$$w^-(x) = \lim_{s \nearrow 0} w(x+s), \qquad w^+(x) = \lim_{s \searrow 0} w(x+s).$$

The following properties of the projection π_h can be found in Appendix C of [18].

Lemma A.5. *The operator $\pi_h : H^1_{pw}(\mathcal{T}_h) \to W_h$ is a well-defined projection. Moreover, for any element $T = (x^{\rm in}, x^{\rm out}) \in \mathcal{T}_h$ and $w \in H^{k+1}_{pw}(\mathcal{E})$, we have $\pi_h w(x^{\rm out}) = w^-(x^{\rm out})$ and*

$$\|w - \pi_h w\|_{L^2(T)} \le C h_T^{k+1} \|w\|_{H^{k+1}(T)}, \tag{A.10}$$
$$\|\partial_x w - \partial_x \pi_h w\|_{L^2(T)} \le C h_T^{k} \|w\|_{H^{k+1}(T)}, \tag{A.11}$$
$$\big|w^+\big(x^{\rm in}\big) - \pi_h w^+\big(x^{\rm in}\big)\big| \le C h_T^{k+1/2} \|w\|_{H^{k+1}(T)}, \tag{A.12}$$
$$|\partial_x w - \partial_x \pi_h w|_{\partial T} \le C h_T^{k-1/2} \|w\|_{H^{k+1}(T)}. \tag{A.13}$$

By the triangle inequality, we can now split the discretization error

$$\|u^\varepsilon(t) - u_h^\varepsilon(t)\|_{L^2(\mathcal{E})} \le \|\eta_h(t)\|_{L^2(\mathcal{E})} + \|e_h(t)\|_{L^2(\mathcal{E})}$$

into a projection error $\eta_h := u^\varepsilon - \pi_h u^\varepsilon$ and a discrete error component $e_h := u_h^\varepsilon - \pi_h u^\varepsilon$. *Via* the estimate of Lemma A.5 and the continuous embedding of $H^1(0,t_{\max}) \subset L^\infty(0,t_{\max})$, we can bound the projection error by

$$\|\eta_h\|^2_{L^\infty(0,t_{\max};L^2(\mathcal{E}))} \le c \sum_{T\in\mathcal{T}_h} h_T^{k+1} \|u^\varepsilon\|^2_{H^1(0,t_{\max};H^{k+1}(T))}.$$

The remaining part of this section is now devoted to the estimation of the discrete error. We denote by $\hat\pi_h : H^1(\mathcal{E}) \to \hat W_h$, $u \mapsto u|_{\mathcal{X}_h\cup\mathcal{V}_0}$ the interpolation of the continuous function u at the interior mesh points. This coincides with the definition of $\hat u^\varepsilon$ in Lemma A.4, and consequently $\hat\eta_h := \hat u^\varepsilon - \hat\pi_h u^\varepsilon = 0$. From the consistency of the scheme stated in Lemma A.4, one can deduce that

$$\begin{aligned}\frac{1}{2}\frac{\mathrm{d}}{\mathrm{d}t}\|e_h\|^2 = (\partial_t e_h, e_h)_{\mathcal{T}_h} &= -b_h(e_h,\hat e_h; e_h,\hat e_h) - \varepsilon d_h(e_h,\hat e_h; e_h,\hat e_h) + (\partial_t\eta_h, e_h)_{\mathcal{T}_h}\\ &\quad + b_h(\eta_h,\hat\eta_h; e_h,\hat e_h) + \varepsilon d_h(\eta_h,\hat\eta_h; e_h,\hat e_h)\\ &= \text{(i)} + \text{(ii)} + \text{(iii)} + \text{(iv)} + \text{(v)}.\end{aligned}$$

With the properties of Lemma A.2, we see that

$$\text{(i)} + \text{(ii)} = -\varepsilon\|\partial_x e_h\|^2_{\mathcal{T}_h} - \varepsilon\left|\left(\frac{\alpha}{h_{\mathrm{loc}}}\right)^{1/2}(e_h - \hat e_h)\right|^2_{\partial\mathcal{T}_h} - \frac{1}{2}\left|b^{1/2}(e_h-\hat e_h)\right|^2_{\partial\mathcal{T}_h}.$$

By Cauchy–Schwarz and Young inequalities, we further obtain

$$\text{(iii)} = (\partial_t u^\varepsilon - \partial_t\pi_h u^\varepsilon, e_h)_{\mathcal{T}_h} \le c\sum_{T\in\mathcal{T}_h} h_T^{2k+2}\|\partial_t u^\varepsilon\|^2_{H^{k+1}(T)} + \frac{1}{2}\|e_h\|^2_{\mathcal{T}_h}.$$

Here, we used the fact that $\partial_t\pi_h u^\varepsilon = \pi_h\partial_t u^\varepsilon$ as well as the projection error estimates of Lemma A.5. For the fourth term we observe that

$$\text{(iv)} = -(b\eta_h, \partial_x e_h)_{\mathcal{T}_h} + \langle nb\,\eta_h^{up}, e_h\rangle_{\partial\mathcal{T}_h} = 0,$$

where the first term vanishes due to (A.9) and the second one due to (A.8) and the definition of $\hat\pi_h$, which together yield $\eta_h^{up} = 0$. Cauchy–Schwarz and Young's inequality as well as a discrete trace inequality finally allow to estimate the last term by

$$\begin{aligned}\text{(v)} \le \varepsilon\|\partial_x e_h\|^2_{\mathcal{T}_h} &+ \varepsilon\left|\left(\frac{\alpha}{h_{\mathrm{loc}}}\right)^{1/2}(e_h-\hat e_h)\right|^2_{\partial\mathcal{T}_h} + \frac{\varepsilon}{2}\|\partial_x\eta_h\|^2_{\mathcal{T}_h}\\ &+ \frac{\varepsilon}{2}\left|\left(\frac{h_{\mathrm{loc}}}{\alpha}\right)^{1/2}\partial_x\eta_h\right|^2_{\partial\mathcal{T}_h} + \frac{\varepsilon}{2}\left(\alpha + C_{tr}^2\right)\left|h_{\mathrm{loc}}^{-1/2}(\eta_h - \hat\eta_h)\right|^2_{\partial\mathcal{T}_h}.\end{aligned}$$

Note that the first two terms cancel with the two last terms in the estimate of (i) + (ii). The remaining terms can again be bounded by the projection error estimates of Lemma A.5, which finally leads to

$$\frac{1}{2}\frac{\mathrm{d}}{\mathrm{d}t}\|e_h\|^2_{\mathcal{T}_h} \le c\sum_{T\in\mathcal{T}_h} h_T^{2k+2}\|\partial_t u^\varepsilon\|^2_{H^{k+1}_{pw}(T)} + c'\sum_{T\in\mathcal{T}_h}\varepsilon h_T^{2k}\|u^\varepsilon\|^2_{H^{k+1}_{pw}(T)} + \frac{1}{2}\|e_h\|^2_{\mathcal{T}_h}.$$

By application of Gronwall's lemma, we thus obtain

$$\|e_h\|^2_{L^\infty(0,t_{\max};L^2(\mathcal{E}))} \le c''\sum_{T\in\mathcal{T}_h}\left(\varepsilon h_T^{2k} + h_T^{2k+2}\right)\|u^\varepsilon\|^2_{H^1(0,t_{\max};H^{k+1}(T))},$$

where we used that $e_h(0) = \pi_h u(0) - u_h(0) = 0$ by definition of the initial values. This already concludes the proof of Theorem 4. □

Acknowledgements. The authors are grateful for financial support from the German Research Foundation (DFG) *via* grant TRR 154, subproject C04, project-number 239904186.

References

[1] G. Akrivis, C. Makridakis and R.H. Nochetto, Galerkin and Runge-Kutta methods: unified formulation, a posteriori error estimates and nodal superconvergence. *Numer. Math.* **118** (2011) 429–456.
[2] J.A. Bárcena-Petisco, M. Cavalcante, G.M. Coclite, N. de Nitti and E. Zuazua, Control of hyperbolic and parabolic equations on networks and singular limits. HAL-report 03233211 (2021).
[3] G. Chen, J.R. Singler and Y. Zhang, An HDG method for Dirichlet boundary control of convection dominated diffusion PDEs. *SIAM J. Numer. Anal.* **57** (2019) 1919–1946.
[4] B. Cockburn, J. Gopalakrishnan and R. Lazarov, Unified hybridization of discontinuous Galerkin, mixed, and continuous Galerkin methods for second order elliptic problems. *SIAM J. Numer. Anal.* **47** (2009) 1319–1365.
[5] G.M. Coclite and M. Garavello, Vanishing viscosity for traffic on networks. *SIAM J. Math. Anal.* **42** (2010) 1761–1783.
[6] P. Constantinou and C. Xenophontos, Finite element analysis of an exponentially graded mesh for singularly perturbed problems. *Comput. Methods Appl. Math.* **15** (2015) 135–143.
[7] D.A. Di Pietro and A. Ern, Mathematical Aspects of Discontinuous Galerkin Methods. Vol. 69. Springer Science & Business Media (2011).
[8] B. Dorn, M. Kramar Fijavž, R. Nagel and A. Radl, The semigroup approach to transport processes in networks. *Phys. D* **239** (2010) 1416–1421.
[9] R.G. Durán and A.L. Lombardi, Finite element approximation of convection diffusion problems using graded meshes. *Appl. Numer. Math.* **56** (2006) 1314–1325.
[10] H. Egger and N. Philippi, A hybrid discontinuous Galerkin method for transport equations on networks, in Finite Volumes for Complex Applications IX, Bergen, Norway, June 2020. Vol. 323 of *Springer Proc. Math. Stat.* Springer, Cham (2020) 487–495.
[11] H. Egger and N. Philippi, On the transport limit of singularly perturbed convection-diffusion problems on networks. *Math. Methods Appl. Sci.* **44** (2021) 5005–5020.
[12] H. Egger and J. Schöberl, A hybrid mixed discontinuous Galerkin finite-element method for convection-diffusion problems. *IMA J. Numer. Anal.* **30** (2010) 1206–1234.
[13] G. Fu, W. Qiu, and W. Zhang, An analysis of HDG methods for convection-dominated diffusion problems. *ESAIM Math. Model. Numer. Anal.* **49** (2015) 225–256.
[14] M. Garavello and B. Piccoli, Traffic Flow on Networks. Vol. 1 of *AIMS Series on Applied Mathematics*. American Institute of Mathematical Sciences (AIMS), Springfield, MO (2006).
[15] E.C. Gartland, Jr., Graded-mesh difference schemes for singularly perturbed two-point boundary value problems. *Math. Comput.* **51** (1988) 631–657.
[16] F.R. Guarguaglini and R. Natalini, Vanishing viscosity approximation for linear transport equations on finite star-shaped networks. *J. Evol. Equ.* **21** (2021) 2413–2447.
[17] S.-A. Hauschild, N. Marheineke, V. Mehrmann, J. Mohring, A.M. Badlyan, M. Rein and M. Schmidt, Port-Hamiltonian modeling of district heating networks, in Progress in Differential-Algebraic Equations II. *Differ.-Algebr. Equ. Forum.* Springer, Cham (2020) 333–355.
[18] V. John, Finite Element Methods for Incompressible Flow Problems. Vol. 51 of *Springer Series in Computational Mathematics*. Springer, Cham (2016).
[19] R.B. Kellogg and A. Tsan, Analysis of some difference approximations for a singular perturbation problem without turning points. *Math. Comput.* **32** (1978) 1025–1039.
[20] C.D. Laird, L.T. Biegler, B.G. van Bloemen Waanders and R.A. Bartlett, Contamination source determination for water networks. *J. Water Res. Plan. Man.* **131** (2005) 125–134.
[21] D. Mugnolo, Semigroup Methods for Evolution Equations on Networks. Springer, Cham (2014).
[22] N.C. Nguyen, J. Peraire and B. Cockburn, An implicit high-order hybridizable discontinuous Galerkin method for the incompressible Navier–Stokes equations. *J. Comput. Phys.* **230** (2011) 1147–1170.
[23] S.F. Oppenheimer, A convection-diffusion problem in a network. *Appl. Math. Comput.* **112** (2000) 223–240.
[24] S.C.S. Rao and V. Srivastava, Parameter-robust numerical method for time-dependent weakly coupled linear system of singularly perturbed convection-diffusion equations. *Differ. Equ. Dyn. Syst.* **25** (2017) 301–325.
[25] H.-G. Roos and T. Linß, Sufficient conditions for uniform convergence on layer-adapted grids. *Computing* **63** (1999) 27–45.
[26] H.-G. Roos and T. Skalický, A comparison of the finite element method on Shishkin and Gartland-type meshes for convection-diffusion problems, in International Workshop on the Numerical Solution of Thin-layer Phenomena (Amsterdam, 1997). Vol. 10 (1997) 277–300.
[27] H.-G. Roos, M. Stynes and L. Tobiska, Robust Numerical Methods for Singularly Perturbed Differential Equations. Vol. 24 of *Springer Series in Computational Mathematics*, 2nd edition. Springer-Verlag, Berlin (2008).
[28] H.-G. Roos, L. Teofanov and Z. Uzelac, Graded meshes for higher order FEM. *J. Comput. Math.* **33** (2015) 1–16.
[29] M. Schmidt, D. Aßmann, R. Burlacu, J. Humpola, I. Joormann, N. Kanelakis, T. Koch, D. Oucherif, M. E. Pfetsch, L. Schewe, R. Schwarz and M. Sirvent, GasLib – a library of gas network instances. *Data* **2** (2017) 40.
[30] G. Singh and S. Natesan, Study of the NIPG method for two-parameter singular perturbation problems on several layer-adapted grids. *J. Appl. Math. Comput.* **63** (2020) 683–705.

[31] M. Stynes and E. O'Riordan, Uniformly convergent difference schemes for singularly perturbed parabolic diffusion-convection problems without turning points. *Numer. Math.* **55** (1989) 521–544.
[32] V. Thomée, Galerkin Finite Element Methods for Parabolic Problems. Vol. 25. Springer Science & Business Media (2007).
[33] Z. Xie and Z. Zhang, Uniform superconvergence analysis of the discontinuous Galerkin method for a singularly perturbed problem in 1-D. *Math. Comp.* **79** (2010) 35–45.

Please help to maintain this journal in open access!

This journal is currently published in open access under the Subscribe to Open model (S2O). We are thankful to our subscribers and supporters for making it possible to publish this journal in open access in the current year, free of charge for authors and readers.

Check with your library that it subscribes to the journal, or consider making a personal donation to the S2O programme by contacting subscribers@edpsciences.org.

More information, including a list of supporters and financial transparency reports, is available at https://edpsciences.org/en/subscribe-to-open-s2o.